Human Molecular Genetics, 2010, Vol. 19, No. 11 **2251–2267**
doi:10.1093/hmg/ddq104
Advance Access published on March 10, 2010

The PCP genes *Celsr1* and *Vangl2* are required for normal lung branching morphogenesis

Laura L. Yates[1], Carsten Schnatwinkel[2], Jennifer N. Murdoch[1], Debora Bogani[1], Caroline J. Formstone[3], Stuart Townsend[1], Andy Greenfield[1], Lee A. Niswander[2] and Charlotte H. Dean[1,*]

[1]Medical Research Council, Harwell, Oxfordshire OX11 0RD, UK, [2]Howard Hughes Medical Institute, Department of Pediatrics, Section of Developmental Biology, University of Colorado Denver School of Medicine, Aurora, CO, USA and [3]MRC Centre for Developmental Neurobiology, Kings College London, New Hunts House, London SE1 1UL, UK

Received February 12, 2010; Revised and Accepted March 8, 2010

The lungs are generated by branching morphogenesis as a result of reciprocal signalling interactions between the epithelium and mesenchyme during development. Mutations that disrupt formation of either the correct number or shape of epithelial branches affect lung function. This, in turn, can lead to congenital abnormalities such as cystadenomatoid malformations, pulmonary hypertension or lung hypoplasia. Defects in lung architecture are also associated with adult lung disease, particularly in cases of idiopathic lung fibrosis. Identifying the signalling pathways which drive epithelial tube formation will likely shed light on both congenital and adult lung disease. Here we show that mutations in the planar cell polarity (PCP) genes *Celsr1* and *Vangl2* lead to disrupted lung development and defects in lung architecture. Lungs from *Celsr1*^{Crsh} and *Vangl2*^{Lp} mouse mutants are small and misshapen with fewer branches, and by late gestation exhibit thickened interstitial mesenchyme and defective saccular formation. We observe a recapitulation of these branching defects following inhibition of Rho kinase, an important downstream effector of the PCP signalling pathway. Moreover, epithelial integrity is disrupted, cytoskeletal remodelling perturbed and mutant endoderm does not branch normally in response to the chemoattractant FGF10. We further show that Celsr1 and Vangl2 proteins are present in restricted spatial domains within lung epithelium. Our data show that the PCP genes *Celsr1* and *Vangl2* are required for foetal lung development thereby revealing a novel signalling pathway critical for this process that will enhance our understanding of congenital and adult lung diseases and may in future lead to novel therapeutic strategies.

INTRODUCTION

Lung diseases, both congenital and late onset, represent a significant clinical burden, and current treatments available are often limited and only partially effective. Defects in lung development result in a range of human disorders including: cystadenomatoid malformations, pulmonary hypertension and agenesis or hypoplasia of the lung (1–3). Importantly, efficient post-natal lung function requires the generation of normal cell and tissue architecture *in utero* (3). In adult lung diseases such as idiopathic pulmonary fibrosis and adult respiratory distress syndrome one of the dominant features is fibrosis (4); which results in abnormal tissue structure leading to impaired gas/air exchange and respiratory dysfunction.

Development of the lung and other branched organs, is driven by signalling between the mesenchyme and epithelium which directs the growth and patterning of buds. Through the study of mouse mutants, a number of these signals that coordinate branching morphogenesis have been identified including members of the FGF, BMP and Wnt growth factor families (5–8). Moreover, complex morphogenetic movements are required to form and precisely shape the networks of three-dimensional (3D) epithelial tubes within the lung and this is achieved through modification of both the

*To whom correspondence should be addressed. Fax: +44 1235 841282; Email: c.dean@har.mrc.ac.uk

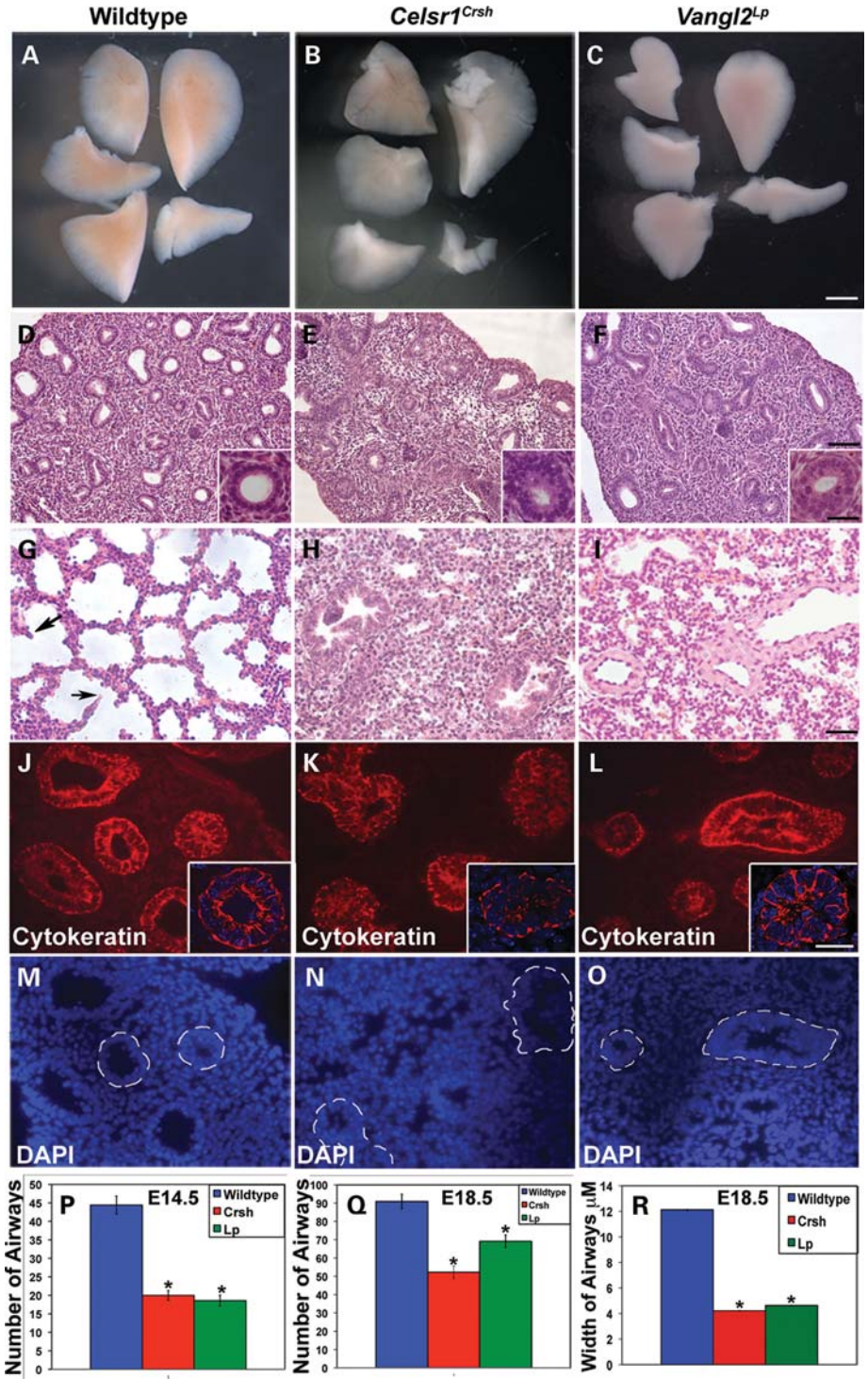

Figure 1. Disruption of *Celsr1* or *Vangl2* causes lung morphogenesis defects. Analysis of E18.5 separated mouse embryonic lung lobes (**A**–**C**) reveals visibly misshapen lung lobes of *Celsr1*^{Crsh} (B) and *Vangl2*^{Lp} (C) lungs compared with wild-type (A). H&E staining of sections of E14.5 *Celsr1*^{Crsh} (**E**) and *Vangl2*^{Lp} (**F**) lungs compared with wild-type (**D**). (**P**) There was a significant reduction in the number of epithelial branches in both mutants at E14.5: wild-type 44.42, $\pm$2.43, $n = 12$; *Celsr1*^{Crsh} 20.00, $\pm$1.3, $n = 12$; *Vangl2*^{Lp} 18.58, $\pm$1.48, n=12. H&E sections from a minimum of three mutants for each genotype were used for counts. Airway lumina were narrow or absent in many *Crsh/Crsh* and *Lp/Lp* airways and epithelium had a multilayered morphology, in contrast to the wider lumina surrounded by single layered epithelium that predominates in wild-type. H&E staining of sections of E18.5 wild-type (**G**), *Celsr1*^{Crsh} (**H**), *Vangl2*^{Lp} (**I**) lungs. Control lung sections display typical saccular structure and evidence of septation (arrows in G). In contrast, mutant lung sections (H, I) show no evidence of septation. Number (**Q**) and width (**R**) of airways is dramatically reduced at E18.5. Number or width of airways was determined by counting airways visible in a complete section of E18.5 lungs from a minimum of two separate embryos (Q) wild-type 90.89, $\pm$3.97; *Celsr1*^{Crsh} 52.22, $\pm$3.37; *Vangl2*^{Lp} 69.11, $\pm$3.43, $n = 9$ for each genotype (R) wild-type 12.13, $\pm$0.05, *Celsr1*^{Crsh} 4.21, $\pm$0.03, *Vangl2*^{Lp} 4.63, $\pm$0.03, $n = 10$ for each genotype. E14.5 cryosections immunostained for expression of pan-cytokeratin (**J**–**L**, inserts show airways at higher magnification), corresponding sections to (J–L) counterstained with DAPI (**M**–**O**), dashed lines outline cytokeratin positive cells (as seen in J–L) difficult to distinguish from surrounding cells in *Celsr1*^{Crsh} (**N**) and *Vangl2*^{Lp} (O), airways are easily visualized in wild-type (M). Scale bars: (A–C) 62.5 μM; (D–F) 50 μM; (G–O) 12.5 μM, inserts in (D–F); (J–L) 5 μM; $^{*}P < 0.05$.

intracellular cytoskeletal network and intercellular interactions like cell adhesion. However, the signalling pathways directing organization of the cytoskeleton during lung development are not well known. Cytoskeletal remodelling can be mediated by RhoGTPases and Rho kinases and previous studies have shown that Rho kinase inhibition causes a severe reduction of lung branching morphogenesis (9,10). Rho kinase is a downstream effector of a number of signalling pathways including the planar cell polarity (PCP) pathway (11–15), which itself is capable of controlling the organized re-structuring of epithelial tissue during development. Understanding the relationship between the PCP pathway and lung development has been recently highlighted as a key unresolved question in pulmonary biology (16).

The PCP pathway is perhaps best known for directing polarization of cells orthogonal to the axis of apical–basal polarity within the plane of an epithelium. In addition to regulating patterning of external epidermal structures such as wing hair cells in *Drosophila* (17), the PCP pathway is more widely utilized for modifying cellular direction and movement (18–21). The end result of the pathway is polarization of the cytoskeleton which, in turn drives cellular morphogenesis and/or morphogenetic movement such as convergent extension. Recent studies show that this pathway can also mediate directed movement of groups of cells and is required for female reproductive tract development and kidney tubule formation (22–24). We hypothesized that the cellular arrangements necessary for lung epithelial tube formation could be coordinated, in part, by the PCP signalling pathway to regulate tissue morphogenesis. Previous studies have shown that *Celsr1* and *Vangl2* are key components of the mammalian PCP signalling pathway (20,21,25). Moreover, mouse mutants of both these genes show extensive phenotypic similarities such as craniorachischisis and disrupted orientation of stereocilia in the cochlea (20,21). We therefore sought to determine whether this signalling pathway is required for lung epithelial tube formation using the previously identified mouse mutants *Celsr1*^{Crsh} and *Vangl2*^{Lp}.

In summary, our manuscript reports the novel finding that mutations in the PCP-related genes *Celsr1* and *Vangl2* result in smaller lungs with a reduced number of epithelial branches, disordered cellular arrangements and, frequently, narrow or absent lumina. This lung phenotype is characterized by disruption of the actin-myosin cytoskeleton in both *Celsr1*^{Crsh} and *Vangl2*^{Lp} and we identify an additional role for Celsr1 in bud bifurcation. We therefore propose that the PCP signalling pathway is required for normal lung branching morphogenesis and that disruption of this pathway leads to defective tissue morphogenesis likely caused by cytoskeletal defects.

RESULTS

Lung morphogenesis is disrupted in *Celsr1*^{Crsh} and *Vangl2*^{Lp} mutants

We examined lungs taken from two mouse mutants which carry loss of function mutations affecting the following proteins: Celsr1 (*crash*, *Crsh*) and Vangl2 (*loop-tail*, *Lp*) (26–30). Briefly, we observed smaller, misshapen lobes and fewer airways with narrow or absent lumina in both *Celsr1*^{Crsh} and *Vangl2*^{Lp} mutants.

Specifically, macroscopic analysis of *Celsr1*^{Crsh} and *Vangl2*^{Lp} homozygotes revealed that mutant lungs were smaller than wild-type littermates, most strikingly, the topology of the lungs was often highly disturbed suggesting that in the absence of *Celsr1* and *Vangl2*, the lung lobes were not able to attain their normal shape (Fig. 1A–C). Analysis of sections of E14.5 *Celsr1*^{Crsh} and *Vangl2*^{Lp} homozygous mutant lung stained with H&E (Fig. 1E and F) revealed changes to the structure of the epithelium from that observed in wild-type lung (Fig. 1D). During normal lung development, airway lumina are initially very narrow and are surrounded by multilayered/pseudostratified type epithelium. As development proceeds, the lumina widen and epithelial thickness subsequently decreases. In wild-type lung sections at E14.5, most airways contained clearly visible lumina surrounded by a single layer of uniformly aligned columnar epithelium (Fig. 1D and insert). However, in both *Celsr1*^{Crsh} and *Vangl2*^{Lp} homozygous lungs the majority of lumina were considerably narrower and the luminal space often contained cells (Fig. 1E, F and inserts). In addition, the surrounding epithelial cells were frequently multilayered and/or disorganized and not aligned uniformly. Although the phenotypes were broadly similar in both mutants, it was notable that *Celsr1*^{Crsh} airways were frequently narrower and cells appeared more densely packed than those in *Vangl2*^{Lp}.

At E18.5 hypoplasia was evident in mutant lungs (Fig. 1H and I) compared with wild-type (Fig. 1G). Moreover, lungs appeared to lack septation and had thickened interstitial mesenchyme. Quantification of these mutant lungs revealed significantly reduced numbers of airways compared with wild-type at E14.5 and E18.5 (Fig. 1P and Q) as well as decreased width of airways (Fig. 1R).

To further highlight the disordered cellular arrangements in the mutant lungs, we immunostained E14.5 lung sections using a pan-cytokeratin antibody to mark epithelial cells and DAPI to highlight all cell nuclei. Wild-type epithelial cells were readily distinguishable from mesenchyme by both cytokeratin and DAPI labelling. The majority of wild-type airways consisted of an open lumen surrounded by a single layer of uniformly aligned nuclei (Fig. 1J and M). In contrast in both mutants, the epithelial cells appeared highly disorganized and randomly orientated (Fig. 1K, L, N, O) with either small or no lumina (see inserts in Fig. 1K and L compared with J). It was often not possible to distinguish epithelial airways from surrounding mesenchyme by DAPI labelling. *Celsr1*^{Crsh} airways appeared more severely affected than *Vangl2*^{Lp}.

Cell differentiation, proliferation and apoptosis are not affected in *Celsr1*^{Crsh} and *Vangl2*^{Lp} lungs

To begin to determine the cause of the lung tissue defects in *Celsr1*^{Crsh} and *Vangl2*^{Lp} mutants we first looked for evidence of changes in cell differentiation, proliferation and apoptosis. To determine whether epithelial cell differentiation was affected in the mutants, we performed immunohistochemistry on E18.5 *Crsh/Crsh* (Fig. 2B and E) and *Lp/Lp* (Fig. 2C and F) mutant lungs using α-smooth muscle actin, to highlight smooth muscle cells surrounding proximal airways, and pro-surfactant protein C, a marker of alveolar type II cells in distal airways. We found no major changes in expression of

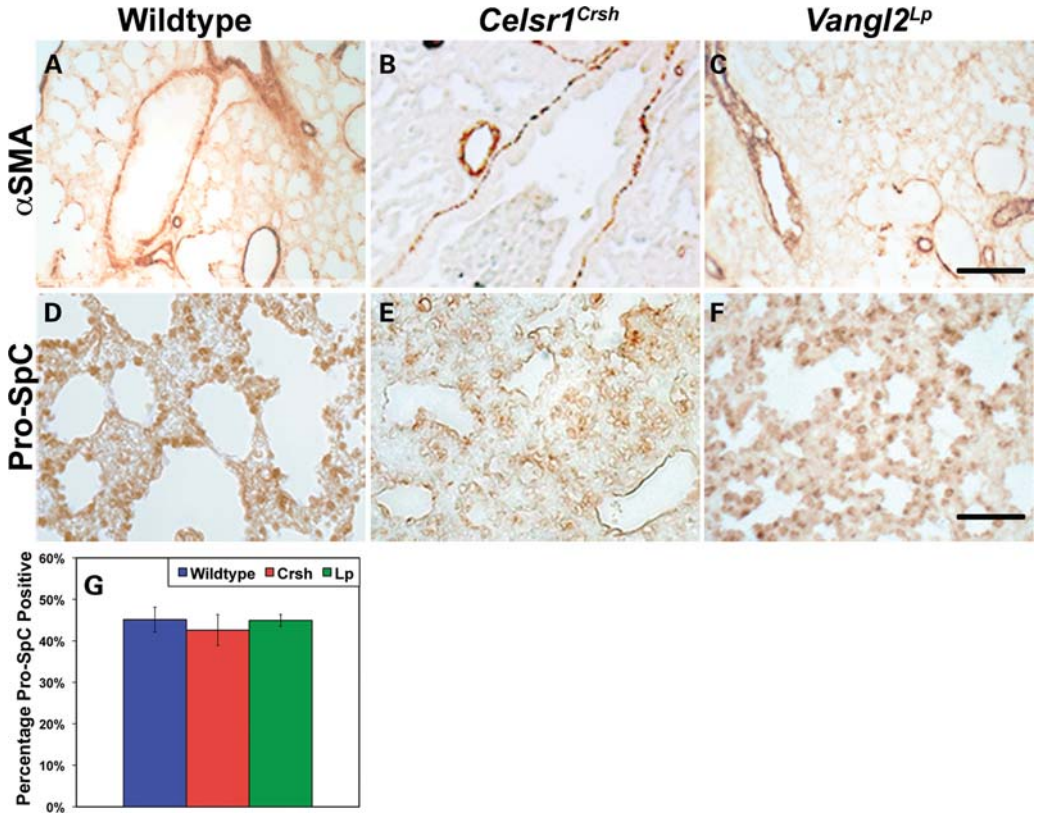

Figure 2. Immunohistochemical analysis of lung epithelial cell differentiation in *Celsr1*^{Crsh} and *Vangl2*^{Lp} compared with wild-type. Comparison of E18.5 control lung sections (**A**, **D**) with *Celsr1*^{Crsh} (**B**, **E**), and *Vangl2*^{Lp} (**C**, **F**) showed no apparent alteration in the expression of proximal airway marker, alpha smooth muscle actin (A–C) or distal airway marker, pro-surfactant C (D–F) Graphical comparison of the percentage of Pro-SP-C positive cells in wild-type and mutant lungs (**G**) confirmed no significant difference between control and *Celsr1*^{Crsh} or *Vangl2*^{Lp} lungs, $n = 8$ for each genotype. Counts were performed on sections of left lung lobe obtained from three mutants for each genotype, $n = 8$ for each genotype. Wild-type 45.12%, ± 3.00; *Celsr1*^{Crsh} 42.60%, ± 3.72; *Vangl2*^{Lp} 44.93%, ± 1.43. Scale bars: (A–F) 12.5 μM.

these markers compared with wild-type littermates (Fig. 2A and D). However, the disrupted tissue architecture in *Celsr1*^{Crsh} and *Vangl2*^{Lp} made detailed comparison of Pro-SpC staining in wild-type and mutant lungs difficult. To circumvent this issue, we compared the percentage of Pro-SpC positive cells in wild-type, *Celsr1*^{Crsh} and *Vangl2*^{Lp} lungs at E18.5 and no significant difference was observed (Fig. 2G). Comparison of a further two cell type specific markers (CC-10 for Clara cells and Aquaporin-5 for alveolar type I cells) also showed no obvious difference between wild-type and mutants (data not shown). We then compared the percentage of proliferating cells in E14.5 wild-type and mutant lung sections to determine whether the reduced number of airways was due to lack of tissue growth. Importantly, there was a comparable percentage of proliferating cells in wild-type, *Celsr1*^{Crsh} and *Vangl2*^{Lp} (Supplementary Material, Fig. S1A–C and H). Similarly, no change in the level of apoptosis was observed in *Celsr1*^{Crsh} or *Vangl2*^{Lp} homozygous lungs (Supplementary Material, Fig. S1D–F). We also saw no changes in proliferation or apoptosis in either mutant at E11.5 when mutants are morphologically indistinct from wild-type (Supplementary Material, Fig. S1G and I). The absence of changes in cell differentiation, proliferation or apoptosis suggests that the cellular disorganization observed in *Celsr1*^{Crsh} and *Vangl2*^{Lp} mutants is caused by impaired cell and tissue morphogenesis. Taking this data into account, we hypothesize that the smaller size of mutant lungs is due to the reduced width and number of lumina and increased compaction of the tissue.

Branching morphogenesis defects in *Celsr1*^{Crsh} and *Vangl2*^{Lp} *ex vivo* lung culture

The predominant driver of lung morphogenesis prior to E16.5 is branching morphogenesis, the process whereby the simple epithelial tube splits into numerous smaller tubes to form the vast number of airways. As airway number is significantly reduced at E14.5 in the mutant lungs, we hypothesized that PCP function is required for lung bud branching. Homozygous *Celsr1*^{Crsh} and *Vangl2*^{Lp} mutant embryos do not exhibit developmental delay as assessed by limb development, however, the rostrocaudal axis is markedly shorter due to disruption of axial convergent extension (31,32). The shortened axis likely results in reduced intrathoracic space, which can affect lung development (33). To circumvent space restriction, we used *ex vivo* culture of E11.5 lungs from intercrosses between *Celsr1*^{Crsh} or *Vangl2*^{Lp} heterozygotes and examined homozygous mutant and wild-type lungs at 0 and 48 h. Bud number in wild-type and mutant lungs was the same at the beginning of branching morphogenesis, $t = 0$ (Fig. 3A–C). However, after

48 h in culture the mutant lungs were smaller with significantly fewer terminal buds than wild-type littermates resulting in a simpler epithelial tree structure (Fig. 3D–F and G). Moreover, terminal buds were significantly enlarged (dashed lines in Fig. 3E and F compared with Fig. 3D, quantification in Fig. 3H). These results indicate that *Celsr1* and *Vangl2* are required for normal lung branching morphogenesis and disrupted branching in mutant lungs is not a consequence of space restriction.

Celsr1 and Vangl2 are required for all three modes of lung branching

Recent studies identified three modes of branching in mouse lung: domain branching, planar bifurcation and orthogonal bifurcation (34). These three modes of branching are used repeatedly to form a stereotypical pattern of branches in the lung. Domain branching is particularly used during the early stages of branching and involves new bud formation at regular intervals both along the length and around the circumference of an existing branch creating a 'bottle-brush' type of structure. Planar and orthogonal bifurcation both involve a single bud tip separating into two distinct tips that are either within the same plane (planar) or at right angles (orthogonal) to the original end bud (see Metzger *et al*. 34 for further details). To determine whether mutations in the PCP pathway affected all branching modes or whether PCP signalling is part of the molecular mechanisms controlling formation of branches by one particular mode, we immunostained wild-type E12.5 and E14.5 whole lungs with antibodies to Celsr1 or Vangl2 and counterstained with pan-cytokeratin to highlight epithelium (Fig. 4, yellow, red, white lines denote planar, domain and orthogonal branching, respectively). Laser scanning confocal examination of wild-type lungs revealed Celsr1 and Vangl2 expression in all three branch modes (Fig. 4B, E, F and H). In addition, despite the defects already described and in particular the decreased branch number, examples of all three modes of branching were visible in $Celsr1^{Crsh}$ and $Vangl2^{Lp}$ homozygous lungs (Fig. 4C, D and data not shown) providing further evidence that *Celsr1* and *Vangl2* are part of a general mechanism governing bud/branch formation.

$Celsr1^{Crsh}$ and $Vangl2^{Lp}$ mutant lungs phenocopy lungs treated with Rho kinase inhibitor and Rho activation partially rescues the branching defect in *Crsh*

Rho kinases are key downstream effectors of the PCP pathway. Previous studies have shown that Rho kinases are important mediators of cellular morphogenesis; they facilitate cytoskeletal remodelling, play an obligatory role in embryonic morphogenesis and are required for normal lung branching morphogenesis (10,35,36). To investigate whether Rho kinase may be part of the downstream signalling pathway utilized by *Celsr1* and *Vangl2* in lung development, we explanted lungs from wild-type mice and cultured them with Rho kinase inhibitor (Y27632) (32,37). We observed a dose-dependent inhibition of branching morphogenesis and enlarged terminal buds (Fig. 3I and L) as reported previously (9). Importantly the phenotype following Rho kinase inhibition is very similar to the phenotype of $Celsr1^{Crsh}$ and $Vangl2^{Lp}$ lungs both in culture and *in vivo*. Moreover, common to both mutants and wild-type lungs treated with Y27632, direct disruption of the actin cytoskeleton with Cytochalasin D also resulted in fewer and broader buds (Fig. 3J and M). Neither Y27632 nor Cytochalasin D adversely affected cell survival, as assessed by comparing the number of fragmented nuclei in control and treated explants following DAPI staining of explants post-culture (Supplementary Material, Fig. S2A–C). Notably, addition of the Rho activator CNF-1 (38) to wild-type lung explants stimulated branching morphogenesis, resulting in an increased number of buds (Fig. 3N).

In a separate set of experiments, the addition of CNF-1 to *Crsh/Crsh* mutant lungs also led to an increase in bud numbers (Fig. 3K and N). The increase in bud numbers was greater in *Crsh/Crsh* lungs than in wild-type (24% increase in *Crsh/Crsh* compared with 16% increase in wild-type Fig. 3N) indicating that activating the Rho signalling pathway in mutant embryos is able to partially ameliorate the branching defect. These data are consistent with Rho kinase being a downstream effector of the PCP signalling pathway in lung development. Thus, we propose that the defective cellular organization in $Celsr1^{Crsh}$ and $Vangl2^{Lp}$ mutants results from disruption to Rho kinase function which likely leads to cytoskeletal defects, thus perturbing tissue structure.

Mutations in *Celsr1* and *Vangl2* lead to disrupted cytoskeletal organization and disordered epithelial airways

To further investigate the hypothesis that Celsr1 and Vangl2 may influence tissue morphogenesis by affecting cytoskeletal organization, we analyzed the appearance of the actin-myosin cytoskeleton and adherens junctions in E14.5 lung tissue. Phalloidin staining of F-actin highlighted the disorder amongst cells in mutant tissue. In wild-type tissue, staining was visible around the entire circumference of cells, this was particularly evident in mesenchyme; in epithelial airways, a strong band of actin was visible surrounding the lumen (Fig. 5A). However, in $Celsr1^{Crsh}$ and $Vangl2^{Lp}$ lung tissue, actin was more discontinuous and diffuse around the circumference of many cells and we did not observe a distinct band of actin surrounding the narrower mutant lumina (Fig. 5B and C). At E18.5, phalloidin staining continued to reveal differences in the F-actin cytoskeleton of wild-type and mutant lung tissue. In wild-type lung, areas of focal enrichment of actin were observed within individual cells throughout the tissue, particularly in cells adjacent to airways (Fig. 5D). In both mutants, localized enrichment of actin was observed in some cells, however, this was either distributed evenly around the entire circumference of cells in $Celsr1^{Crsh}$ (Fig. 5E) or was discontinuous and diffuse in $Vangl2^{Lp}$ (Fig. 5F). Moreover, in both mutants, those cells which did display focal enrichment of actin were frequently not adjacent to 'airways'. Levels of non-muscle myosin II, another critical component of the cytoskeleton which directly links the Rho signalling pathway with cytoskeletal dynamics (39), were also perturbed and its spatial distribution altered at E14.5 in $Celsr1^{Crsh}$ and $Vangl2^{Lp}$ mutants (Fig. 5H and I; wild-type in G). In common with our earlier observations,

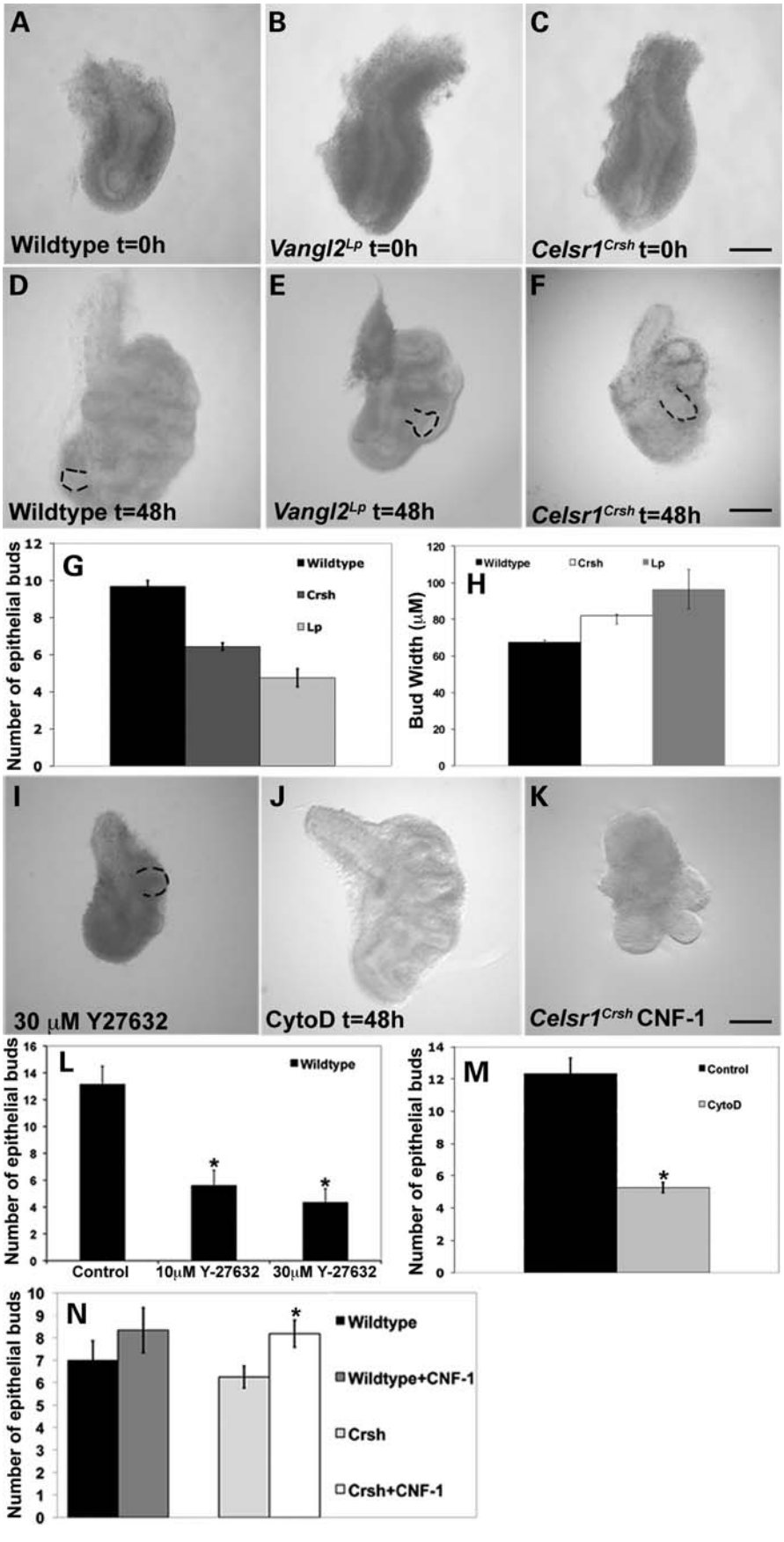
A
Wildtype t=0h
B
Vangl2Lp t=0h
C
Celsr1Crsh t=0h
D
Wildtype t=48h
E
Vangl2Lp t=48h
F
Celsr1Crsh t=48h
G
Number of epithelial buds
Wildtype
Crsh
Lp
H
Bud Width (μM)
Wildtype
Crsh
Lp
I
30 μM Y27632
J
CytoD t=48h
K
Celsr1Crsh CNF-1
L
Number of epithelial buds
Wildtype
Control
10μM Y-27632
30μM Y-27632
M
Number of epithelial buds
Control
CytoD
N
Number of epithelial buds
Wildtype
Wildtype+CNF-1
Crsh
Crsh+CNF-1

both F-actin and myosin appeared considerably more disrupted in *Celsr1*^{Crsh} than in *Vangl2*^{Lp}. The cytoskeletal defects observed in *Celsr1*^{Crsh} and *Vangl2*^{Lp} lungs might be expected to cause disruption of adherens junctions, however, staining with anti-β-catenin antibody (Fig. 5J–L) showed no apparent changes in *Celsr1*^{Crsh} or *Vangl2*^{Lp} lungs indicating that adherens junctions were not grossly affected.

In light of the aberrant epithelial tube morphogenesis in *Celsr1*^{Crsh} and *Vangl2*^{Lp} lungs, it was important to determine whether apical–basal polarity was disrupted. Immunolabelling with ZO-2 and laminin, to highlight the apical and basal sides of airways, respectively (Fig. 5M–O), as well as with the apical membrane marker aPKCζ (Fig. 5P–R) and GM-130 (Supplementary Material, Fig. S3A–C) to mark the polarized localization of the Golgi apparatus, showed no overt disruption to apical–basal polarity in either mutant. Some differences in the precise patterns of expression of markers was visible in mutants, however, this likely reflects the misalignment of cells, the narrowed lumina and the overall perturbation of tissue morphogenesis, rather than disrupted apical–basal polarity. Thus, mutations in *Celsr1* and *Vangl2* lead to disruption of the cytoskeleton resulting in disordered epithelial airways.

Lung endoderm from *Celsr1*^{Crsh} and *Vangl2*^{Lp} mutants responds to the chemoattractant FGF10 but is unable to branch

We wished to determine whether the tissue morphogenesis defects observed in *Celsr1* and *Vangl2* mutant lungs could reflect a defect in the response of mutant endoderm to a key signal for branching. To test this idea we exposed *Celsr1*^{Crsh}, *Vangl2*^{Lp} and wild-type lung epithelium denuded of mesenchyme to FGF10, which normally signals from the mesenchyme to direct lung branching. Both wild-type and mutant lungs responded to the FGF10 stimulus in terms of growth. However, whereas wild-type epithelium formed multiple long and narrow buds (Fig. 6A and B), in most cases, the mutant lung epithelium did not undergo any branching in response to FGF10 (Fig. 6C, D or rarely one or two short stumpy buds formed). Staining for phospho-ERK1/2, which is up-regulated in response to FGF10 in the lung (40), revealed no significant difference in the number of positive cells in wild-type and mutant lung epithelium and this was confirmed by western blot (Fig. 6E and F). Together these results indicate that the FGF signalling pathway, at least that mediated by ERK1/2 activators, is unaffected in mutant lungs. Thus, normal morphogenetic movement within the epithelium is affected upon disruption of the PCP genes *Celsr1* and *Vangl2*, rendering the epithelium almost incapable of branching in response to an FGF10 stimulus.

Celsr1 and Vangl2 proteins are spatially restricted and differentially expressed in lung epithelia

To provide additional mechanistic insight into how Celsr1 and Vangl2 proteins regulate tissue morphogenesis during lung branching, we next examined their expression patterns in E11.5 and E14.5 lung sections by immunohistochemistry. Studies in other tissues and organisms have shown that these proteins often co-localize at cell membranes and are thought to form a multi-protein complex (20,41). In the lung we did observe co-localization in some regions of lung epithelia but we also noted some differences in the spatial expression of Celsr1 and Vangl2.

At E11.5 at the onset of branching of the secondary buds, Celsr1 expression was mainly restricted to lung epithelium and staining was enriched in the basal membranes as well as towards the more apical side of airways (Fig. 7A). Double immunostaining of Celsr1 with laminin revealed co-localization indicating that Celsr1 was also present in the basement membrane (Fig. 8A–C). This surprising result was confirmed by comparison of the Celsr1 and laminin double labelling with that for laminin and the basolateral membrane marker, β-catenin; no co-localization of β-catenin and laminin was observed since these two proteins are expressed in different compartments (compare Supplementary Material, Fig. S3D–F with H–J). We also noted that basement membrane Celsr1 staining frequently was not evenly distributed around the entire airway and instead was localized to the basement membrane on one side or a portion of the airway, rather than being evenly distributed around it. Interestingly, laminin shares this uneven, differential distribution around the basal side of airways which results from thinning or discontinuity of the basement membrane at the epithelial/mesenchymal interface in regions of active bud outgrowth (42). The co-localization of Celsr1 with laminin in the basement membrane indicated that Celsr1 associates with areas of morphogenetic stability such as clefts (42).

Figure 3. *Ex vivo* lung cultures reveal that mutations in *Celsr1* and *Vangl2* phenocopy treatment with Rho kinase inhibitor and Rho kinase activation partially rescues the branching defect in C*elsr1*^{Crsh}. E11.5 left lung lobes from wild-type (**A**, **D**); *Vangl2*^{Lp} (**B**, **E**) and C*elsr1*^{Crsh} (**C**, **F**) were cultured for 48 h. $t = 0$ mutant lungs (B, C) were indistinguishable from wild-type lungs (A). $t = 48$h wild-type lungs exhibit increased number of terminal buds (D, **G**). A smaller increase in terminal buds is observed in *Vangl2*^{Lp} (E, G) and *Celsr1*^{Crsh} (F, G) explants: wild-type 9.67, ±0.33, $n = 14$; *Crsh* 6.43, ±0.48, $n = 8$; *Lp* 4.75, ±0.2, $n = 6$. Mutant lung buds are also expanded (E, F, **H**) relative to wild-type (D, H): wild-type 67.47, ±4.54, $n = 10$; *Crsh* 81.85, ±4.34, $n = 16$, *Lp* 96.5, ±10.6, $n = 8$. Addition of Y27632 severely inhibits branching morphogenesis of a wild-type lung in a dose dependent manner (**I**, **L**): lung control 13.14, ±0.51, $n = 7$; lung 10 μM Y27632 5.60, ±0.51, $n = 5$; lung 30 μM Y27632 4.33, ±0.42, $n = 6$. Disruption of the cytoskeleton with 100 ng/ml Cytochalasin D also inhibits lung branching morphogenesis (**J**, **M**): wild-type 12.33, ±0.97, $n = 27$; CytoD 5.28, ±0.32, $n = 18$. Explants in (I) and (J) have broad branches and appear similar to those from *Vangl2*^{Lp} (E) and *Celsr1*^{Crsh} (F). Wild-type lung explants treated with 20 ng/ml CNF-1 show a small increase in number of epithelial buds formed (**N**): wild-type (untreated) 7, ±0.94, $n = 6$; wild-type with CNF-1 8.33, ±1.13, $n = 9$, two-tailed P-value = 0.4819. This result was consistent though not statistically significant. Whereas in a separate set of experiments, treatment of *Crsh* homozygous lung explants with 20 ng/ml CNF-1 results in a greater, statistically significant increase in bud numbers (**K**, N): *Crsh* (untreated) 6.25, ±0.52, $n = 8$; *Crsh* with CNF-1 8.18, ±0.63, $n = 11$. Explants were stage matched at $t = 0$ to allow direct comparison of the number of end buds between control and treated or wild-type and mutant lungs within each experiment. Scale bars: (A–F, I–K) 63 μM. *$P < 0.05$.

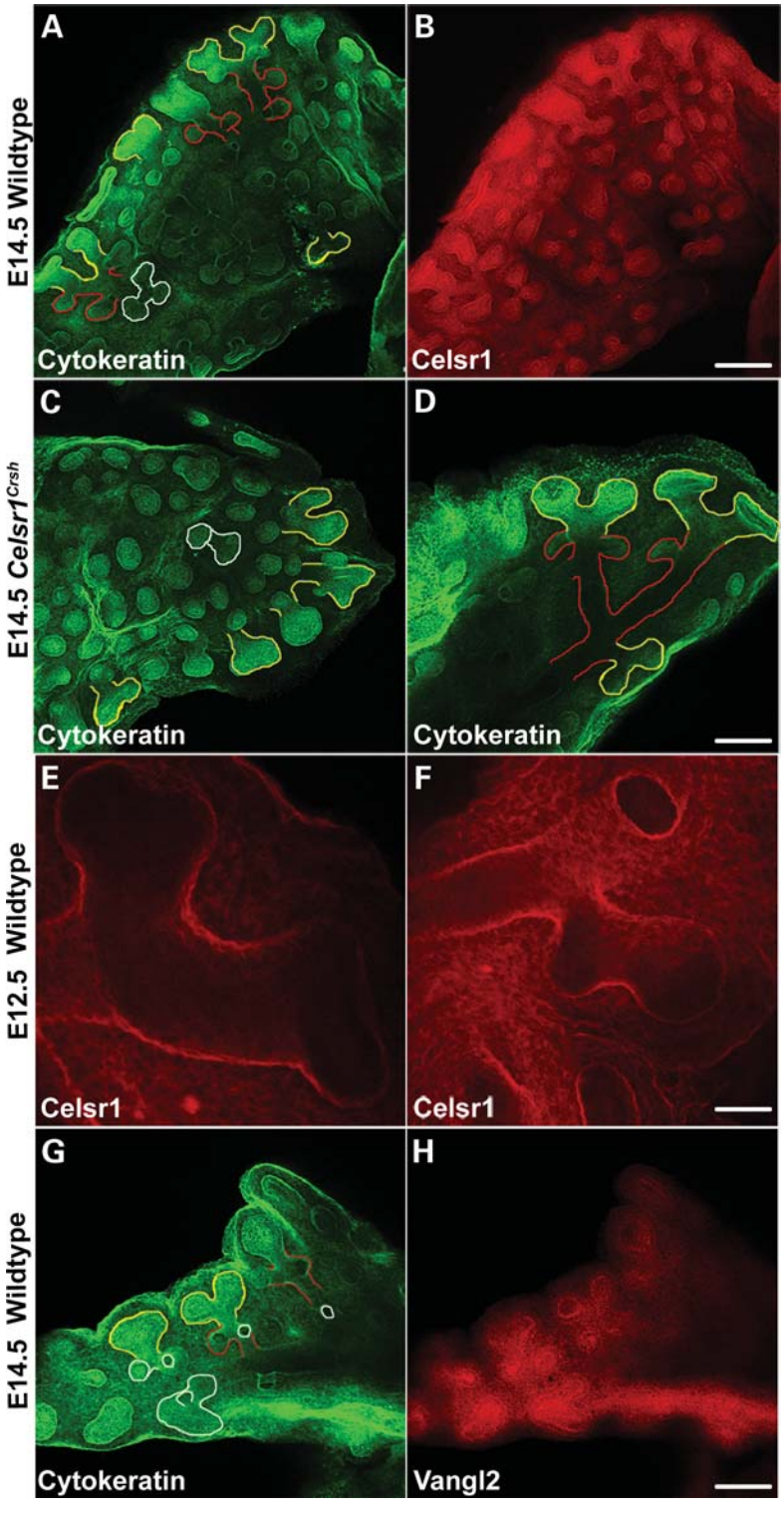

Figure 4. Celsr1 and Vangl2 are expressed in all modes of branching. Confocal images of wild-type E14.5 (**A**, **B**, **G**, **H**) and C*elsr1*^{Crsh} (**C**, **D**) or E12.5 wild-type (**E**, **F**) whole lungs immunostained with anti-cytokeratin (A, C, D, G), anti-Celsr1 (B, E, F) or anti-Vangl2 (H) antibodies. Pictures are slices showing a single layer from a z-stack. In wild-type lungs Celsr1 and Vangl2 are expressed in all three branching modes as described by Metzger *et al*. (34); examples of planar branching (yellow lines in A, C, D, G); domain branching (red lines in A, D, G) and orthogonal branching (white lines in A, C, G) are highlighted. All three modes are present in *Celsr1*^{Crsh} and *Vangl2*^{Lp} lungs (C, D and data not shown) indicating the defects in *Celsr1* and *Vangl2* are not restricted to a specific mode of branching. Scale bars: (A, B) 125 μM plus ×1.2 zoom, (C) 125 μM plus ×1.2 zoom, (D) 125 μM plus ×1.7 zoom. (E, F) 125 μM plus ×6.3 zoom, (G, H) 125 μM plus ×1.7 zoom.

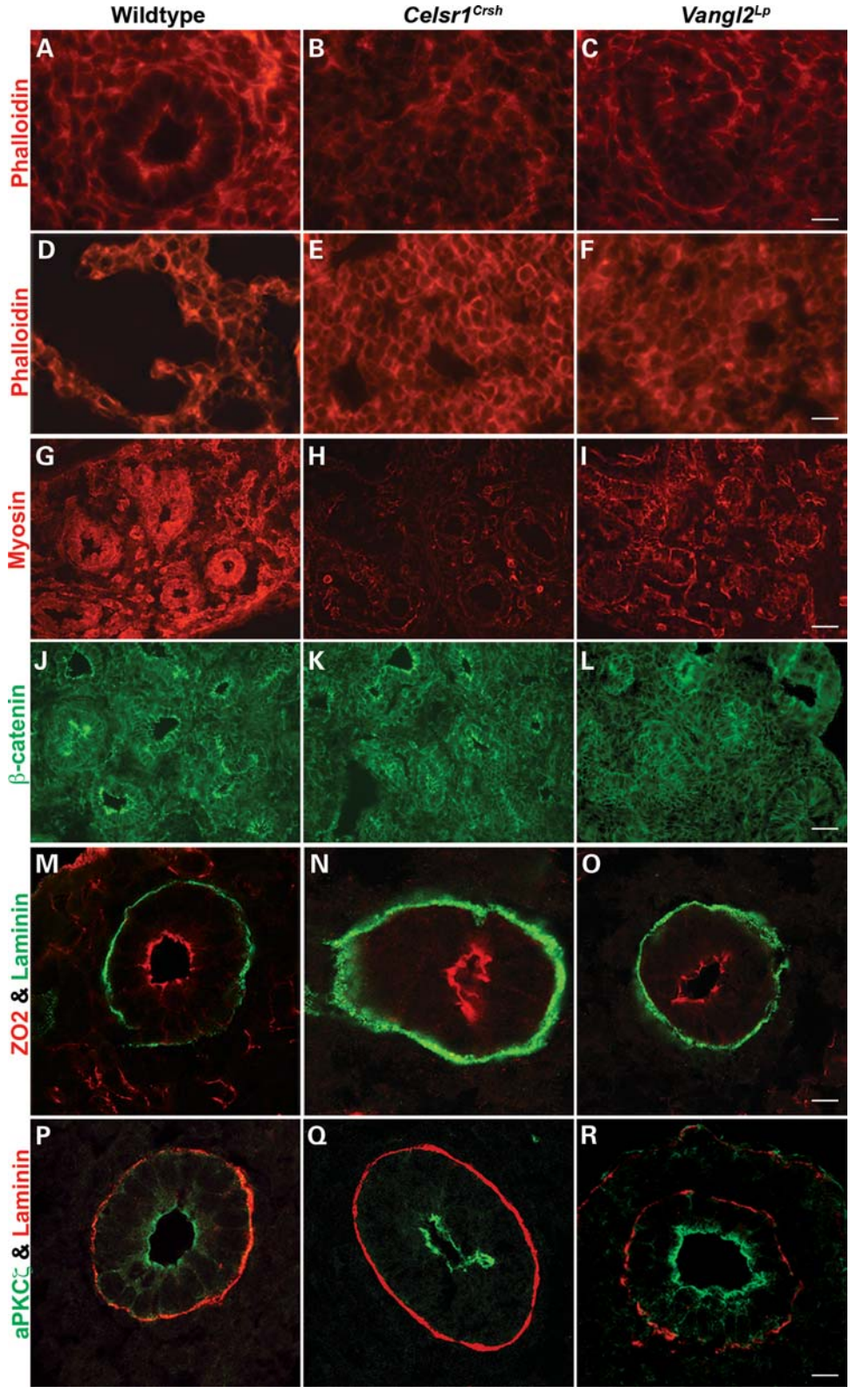

Figure 5. Mutant lungs display aberrant cell architecture, yet apical–basal polarity remains intact. Cryosections of E14.5 wild-type (**A**, **D**, **G**, **J**, **M**, **P**) *Celsr1*^{Crsh} (**B**, **E**, **H**, **K**, **N**, **Q**) and *Vangl2*^{Lp} (**C**, **F**, **I**, **L**, **O**, **R**). Rhodamine phalloidin staining of F-actin reveals cytoskeletal defects in mutants at E14.5 (B, C) and E18.5 (E, F) compared with wild-type (A, D), as does staining with antibodies to non-muscle myosin IIA in mutants (H, I), compared with wild-type (G). Anti-β-catenin staining appears normal in *Celsr1*^{Crsh} (K) and *Vangl2*^{Lp} (L), compared with wild-type (J). Normal apical–basal polarity is revealed in lung by double-labelling of wild-type (M), *Celsr1*^{Crsh} (N) and *Vangl2*^{Lp} (O) airways with ZO-2 (red) and laminin (green in M–O and red in P–R) and by double-labelling of wild-type (P) *Celsr1*^{Crsh} (Q) and *Vangl2*^{Lp} (R) with aPKCζ (green). Scale bars: (A–F) 5 μM, (G–L) 5 μM, (G–L) 25 μM, (M–R) 12.5 μM plus 3× zoom.

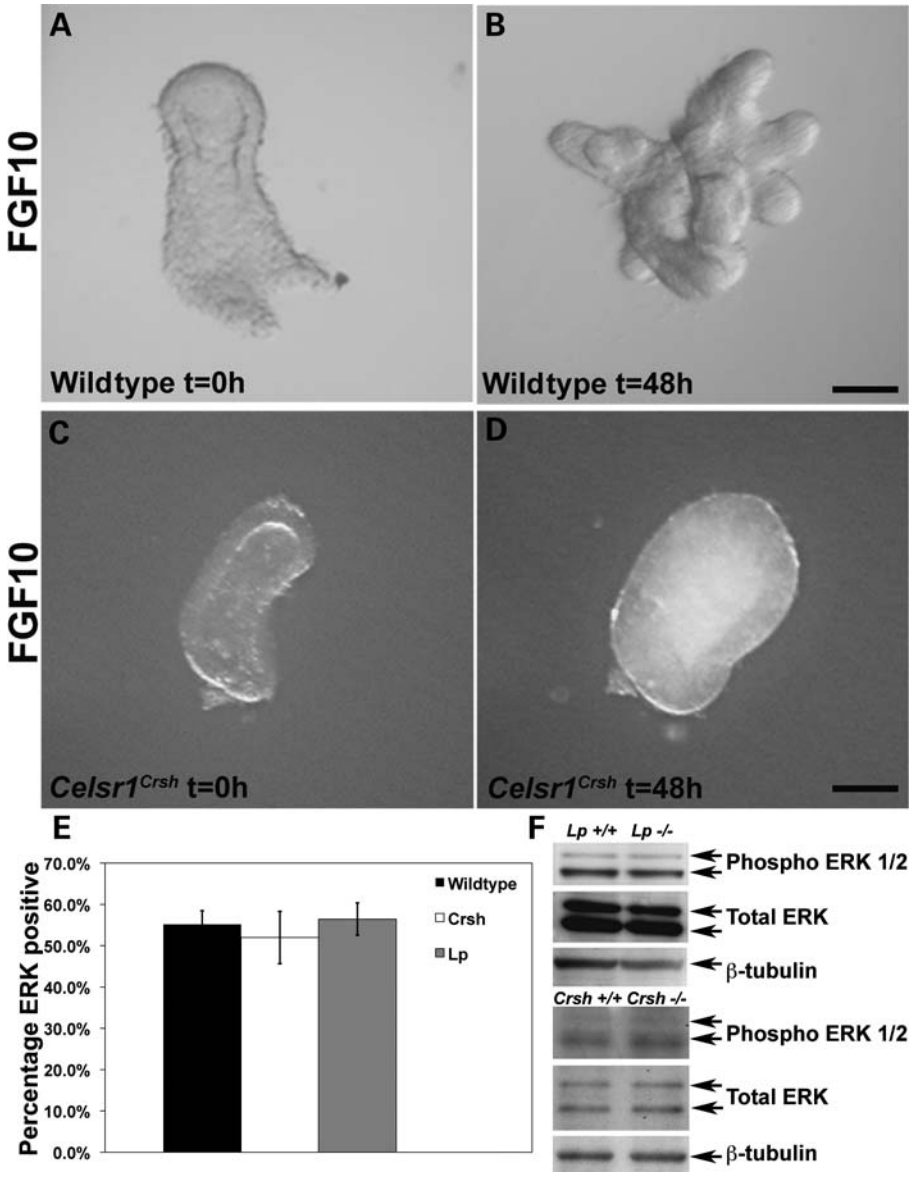

Figure 6. Mutant lung endoderm responds to FGF10 but is unable to undergo branching. (**A**, **B**) Wild-type lung endoderm branches in response to 400 ng/ml FGF10 (mean bud number = 11, $n = 6$). (**C**, **D**) mutant lungs do not branch in response to FGF10 (mean bud number *Crsh* = 0.9, $n = 6$). P-ERK1/2 staining of E14.5 lung, shows no significant difference in percentage of P-ERK1/2 positive cells in the epithelium of mutants compared with wild-type controls (**E**): wild-type 55.17%, ± 3, $n = 10$; *Crsh* 51.97%, ± 6.3, $n = 7$, $P = 0.6074$; *Lp* 56.45%, ± 3.9, $n = 9$, $P = 0.7939$. Data from three embryos for each genotype. Western blotting reveals no change in the relative levels of P-ERK1/2 in wild-type and *Lp/Lp* or *Crsh/Crsh* littermates (**F**). Scale bars: (A–D) 5 μM.

Punctate Vangl2 staining was observed in both epithelium and mesenchyme, though expression in the epithelium was stronger. In the epithelium, Vangl2 staining was more evenly distributed around cell membranes than Celsr1, however, in many airways, we observed an enrichment of Vangl2 expression in cells surrounding the lumen (Fig. 7B), in agreement with a previous study (43).

At E14.5 the patterns of Celsr1 (Fig. 7C) and Vangl2 (Fig. 7E) were similar to E11.5, but the enrichment of Celsr1 towards the luminal side of airways was more predominant. Immunostaining of E14.5 lung sections from homozygous mutants of $Celsr1^{Crsh}$ with anti-Celsr1 (Fig. 7D) and $Vangl2^{Lp}$ with anti-Vangl2 (Fig. 7F) antibodies revealed a dramatic reduction in protein levels in mutant lung tissue relative to wild-type. This demonstrates the specificity of the antibodies and provides supportive evidence that these mutations represent loss of function alleles.

The spatial and temporal distribution of Celsr1 and Vangl2 in lung epithelium clearly overlaps in some regions, such as the apical membranes, but also differs in others, suggesting a differential role for these proteins in some aspects of lung development. This observation prompted us to examine whether Celsr1 was correctly localized in $Vangl2^{Lp}$ mutants and conversely whether Vangl2 was correctly localized in

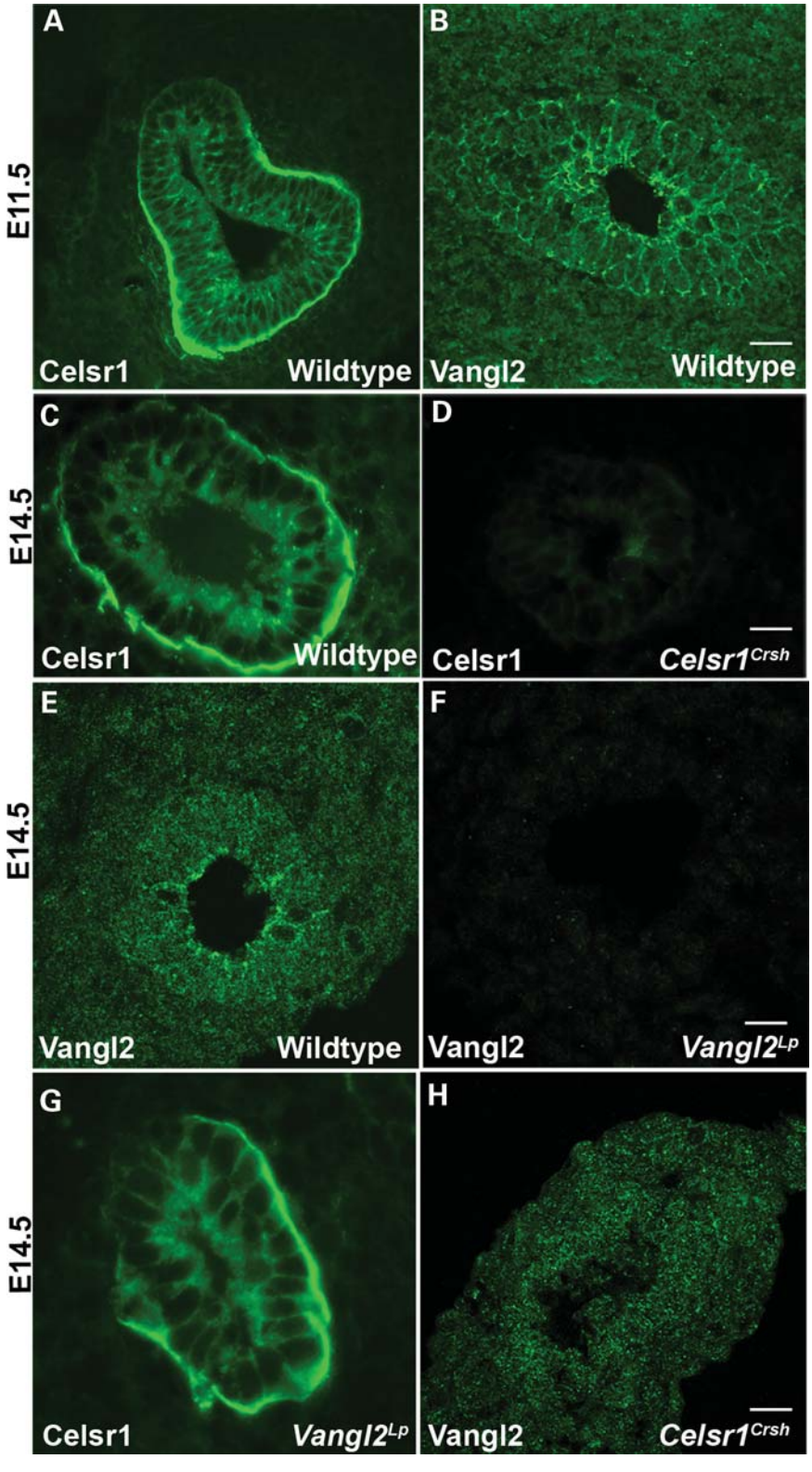

Figure 7. Celsr1 and Vangl2 proteins are spatially restricted and differentially expressed in lung epithelia. (**A**, **B**) E11.5 transverse cryosections of lungs immunostained with antibodies against Celsr1 (A) and Vangl2 (B). (**C**–**F**) Immunostaining of transverse cryosections of E14.5 wild-type (C, E) with anti-Celsr1 (C) and anti-Vangl2 (E) antibodies. Corresponding protein levels are dramatically decreased in lung tissue of mutants; anti-Celsr1 in *Celsr1*^{Crsh} (D) and anti-Vangl2 in *Vangl2*^{Lp} (F) compared with wild-type (C, E). Immunostaining of Celsr1 protein in *Vangl2*^{Lp} (**G**) reveals no change in spatial localization. Enrichment of Vangl2 protein adjacent to the lumen is lost in *Celsr1*^{Crsh} (**H**) mutant lung sections. Scale bars: (A, B) 125 μM plus ×1.9 zoom, (C) 125 μM plus ×2.5 zoom, (D) 125 μM plus ×1 zoom, (E, H) 125 μM plus ×2 zoom, (F, G) 125 μM plus ×3 zoom.

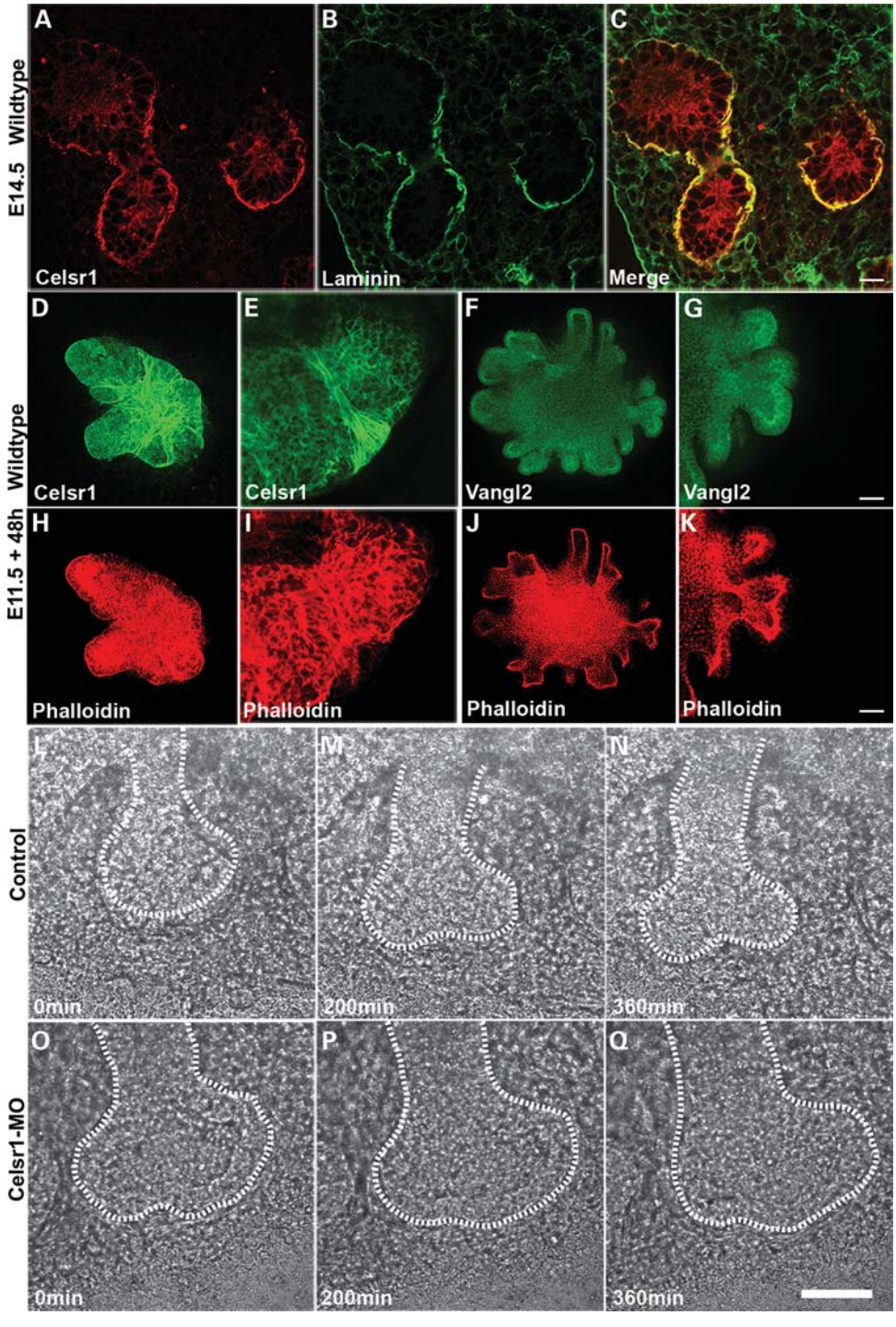

Figure 8. Differential expression of Celsr1 and Vangl2 is observed in branching lung endoderm explants and morpholino knockdown highlights a role for Celsr1 in bifurcation. Double-labelling of wild-type E14.5 cryosections with Celsr1 (**A**, **C**) and laminin (**B**, **C**) antibodies. E11.5 lung endoderm explants cultured for 48 h in 400 ng/ml FGF10 and double labelled with phalloidin (**H**–**K**) and Celsr1 (**D**, **E**) or Vangl2 (**F**, **G**) antibodies. High levels of Celsr1 expression are present in regions of restricted tissue growth such as points of bifurcation (D, E, H, I). Vangl2 is most highly expressed at the luminal surface of outgrowing buds (F, G, J, K). E11.5 lung explants from β-actin promoter driven GFP embryos were cultured for 48 h in the presence of control (**L**–**N**) or Celsr1 (**O**–**Q**) morpholinos and subsequently imaged over a 24 h period. Images show three timepoints from this series. Scale bars: (A–C) 125 μM ×2 zoom (D, H, F, J) 125 μM ×2.7 zoom, (E, I) 125 μM ×10 zoom, (G, K) 125 μM ×8 zoom, (L–Q) 50 μM.

Celsr1^{Crsh} mutants. In *Lp/Lp* lungs, the spatial distribution of Celsr1 did not appear to be altered (Fig. 7G). In contrast, we observed a loss of enrichment of Vangl2 in cells adjacent to the lumen in *Crsh/Crsh* lungs (Fig. 7H) suggesting that Celsr1 is required for this enrichment of Vangl2. Thus, despite differences in Celsr1 and Vangl2 expression patterns, mutations in Celsr1 affect the localization of Vangl2, suggesting an interaction between these proteins in lung.

Celsr1 and Vangl2 expression is enriched in highly specific regions of the branching lung epithelium

Lung branching morphogenesis is a complex 3D process that depends on interactions between the mesenchyme and the epithelium. However, it is possible to simplify this system by culture of the lung endoderm denuded of mesenchyme in the presence of FGF10 to induce branching. In this way, we can gain a better 3D view of the spatial expression of both Celsr1 and Vangl2 in the endoderm during the branching process. Specifically, wild-type lung endoderm explants denuded of mesenchyme were cultured with FGF10 to induce branching and subsequently immunostained for Celsr1 or Vangl2 and phalloidin to detect F-actin cytoskeleton (Fig. 8D–K). This 3D view of branching endoderm revealed dramatic differences in the expression patterns of Celsr1 and Vangl2. Low levels of both proteins were observed in membranes of epithelial cells, imaging through z-stacks of endoderm explants revealed clear enrichment of Vangl2 at the apical/luminal surface of epithelial buds (Figs 8F, G, J, K and 4H). Celsr1 was also enriched towards the luminal surface of buds but in addition, high levels of Celsr1 were detected in the basement membrane, in regions of restricted tissue growth, e.g. immediately adjacent to a bud or at sites of bud bifurcation (Figs 8D, E, H, I and 4E and F) These data confirm what we had previously observed both in lung sections (Fig. 7A–C and E) and with wholemount antibody staining of lungs (Fig. 4B, E, F, H) and strengthen the idea that the functions of Celsr1 and Vangl2 are not completely overlapping.

Morpholino knockdown reveals a role for Celsr1 in bud bifurcation

Given the intriguing expression pattern of Celsr1 in the basement membrane surrounding lung endoderm, we sought to understand more precisely how *Celsr1* affects branching morphogenesis. To do this, we conducted time-lapse imaging of E11.5 wild-type lung explants in the presence of one of two Celsr1 morpholinos (MO) directed against different Celsr1 sites, or control morpholino. Identical results were obtained with both Celsr1 MOs. Knockdown efficiency was validated by immunostaining and western blotting (Supplementary Material, Fig. S4).

Wild-type lungs cultured with control MO exhibited a reproducible branching pattern in culture. The process of branching began with a uniform increase in distal bud size followed by bifurcation (Fig. 8L–N). During bifurcation, the two sides of the bud branched and grew outwards, whereas cells in the middle were constrained and remained in place. In contrast, lungs cultured with Celsr1 MO formed greatly expanded 'fat' buds and bifurcation into two new buds did not occur (Fig. 8O–Q). In Figure 8L and O, a single bud is shown for both Control and Celsr1-MO at $t = 0$. In the control, a cleft forms by 200 min (Fig. 8M) and is in the same position and deeper by 360 min (Fig. 8N). At $t = 0$ in in the Celsr1 MO treated culture (Fig. 8O), a deformity in the epithelial bud is visible but this is not retained in the same position in the bud at 200 or 360 min (Fig. 8P and Q). Moreover, the deformity/apparent cleft does not deepen showing that this is not the beginning of bifurcation. Considerable movement of the epithelial sheet occurs in the Celsr1 MO treated explants resulting in a looser/uneven bud shape. In some buds, after considerable delay, multiple small new buds formed randomly in a non-stereotypical fashion. The absence of properly co-ordinated bifurcation of distal lung buds treated with Celsr1 MO coupled with our protein localization data indicates that Celsr1 is required for bifurcation during the branching process.

DISCUSSION

Mutations in PCP genes disrupt branching morphogenesis and cytoskeletal organization

The complex interactions that enable formation of 3D branched organs are still poorly understood, despite being essential to an understanding of the pathobiology of many diseases and congenital malfomations. This study demonstrates a previously undiscovered role for two genes in the PCP pathway in the control of lung branching morphogenesis. Our data show that mutations in *Celsr1* and *Vangl2* disrupt lung bud branching and cause abnormal epithelial cell arrangements, cytoskeletal defects and lead to narrowed airways and hypoplasia of the lungs. These branching defects can be mimicked by inhibition of Rho kinase, a known downstream effector of PCP and key regulator of the cytoskeleton (12,44,45) and the branching defect can be partially rescued in mutant lung explants by Rho stimulation. We find that despite being competent to respond to FGF10 signalling, *de novo* bud formation is severely impaired in mutant lung endoderm. Importantly, apical–basal polarity appears largely unaffected in mutant lungs. Our studies demonstrate that lung branching morphogenesis requires Celsr1 and Vangl2 function, emphasizing a new role for these proteins during development. Interestingly mutations in two other PCP genes, *Scribble* and *PTK7*, also cause similar lung defects (Yates *et al*. and Paudyal *et al*., manuscripts in preparation). Ultimately, these mutant lung deficiencies are likely to cause acute breathing difficulties (7) and almost certainly, death, although this was not possible to demonstrate due to neonatal death as a result of other tissue defects.

Although mutations in these genes do not prevent branching morphogenesis completely, they do lead to a reduction in the number of branches and major alterations to the shape of branches that are able to form. This level of impact on branch formation is consistent with that seen in mouse mutants of other genes required for branching morphogenesis (46–50). Our results in the early lung (lung explant and Celsr1 morpholino experiments) show an expansion in the size of the bud, yet in the E14.5 and E18.5 lung, the airway lumen is considerably narrowed. The lumen narrowing likely reflects the disorganization of the airway epithelium and may also suggest an inability to maintain the cytoskeletal integrity and lumenal structure resulting in a collapse of the airway. The airway narrowing also likely contributes to the reduction in the size of the later embryonic lung.

Here we have shown that components of the PCP signalling pathway play a critical role in lung epithelial tube formation. The PCP signalling pathway regulates a number of different types of cellular behaviours during development; it is currently

unclear whether any of these are affected in lung development. In vertebrates, PCP signalling regulates convergent extension movements whereby intercalation of cells enables elongation and narrowing of tissues, including rearrangement of the neural plate during neurulation. Recent studies in the kidney have shown that convergent extension occurs during kidney tubule formation and that this process is mediated via the PCP pathway (24). However, *ex vivo* culture of Celsr1 and Vangl2 homozygous lungs reveals broader, but not shorter, epithelial buds compared with wild-type. In addition, morpholino knockdown experiments and time-lapse imaging revealed the tissue is still able to elongate and extend to form 'stalk' regions, thereby suggesting the branching defects are not caused by failure of tissue extension. This is not altogether surprising given that elongation of the epithelial tubes is much more modest in lung compared with that in kidney. Other work in the kidney showed that disruption of PCP leads to randomization of the orientation of cell division that in turn causes dilation of tubules and formation of cysts, a major cause of ciliary disease (51–53). It now appears that both of these cellular behaviours are important in the kidney and that tubule diameter is first established by convergent extension during embryogenesis but is then maintained by polarized cell divisions after birth (24). Other laboratories have highlighted the role of the PCP signalling pathway for proper morphogenesis of a tissue in a number of other distinct sites including heart morphogenesis, formation of the female reproductive tract and directed cell migration *in vitro* (22,54–58). Future studies will be required to determine whether any of these cellular behaviours are disrupted in *Celsr1*^{Crsh} and *Vangl2*^{Lp} lungs.

The expression patterns of Celsr1 and Vangl2 suggest both common and differential roles for these proteins in lung branching morphogenesis

Most studies of PCP proteins emphasize their similar roles in tissue development and frequently note their overlapping expression patterns. In the lung, we observe asymmetric enrichment of Celsr1 and Vangl2 towards or adjacent to the lumen, respectively. Together with the absence or reduced diameter of lumina observed in many *Celsr1*^{Crsh} and *Vangl2*^{Lp} 'airways', this suggests that in common with other apically enriched proteins, Celsr1 and Vangl2 may have an important role in establishing a proper lumen i.e. they may help to modulate co-ordinated cellular movement via regulation of the cytoskeleton that is required for the formation of a normal lumen. Interestingly, analysis of Vangl2 expression in *Crsh* mutants showed a distinct loss of Vangl2 enrichment adjacent to the lumen, suggesting that Celsr1 is required to correctly localize Vangl2. We also noted that the phenotype in *Celsr1*^{Crsh} was consistently more severe than that of *Vangl2*^{Lp}. It is of note that Celsr1 has previously been proposed to exist at the top of a hierarchy of PCP proteins, helping to recruit other PCP proteins to the cell membranes (55,56) and our data are consistent with this view.

In addition to some areas of overlapping expression, we found intriguing differences in expression of Celsr1 and Vangl2 that likely reflect some differing functions. Celsr1 is highly expressed between buds as well as at sites where bifurcation occurs and MO knockdown revealed that Celsr1 is indeed required for normal bud bifurcation. In contrast, Vangl2 is not enriched at sites of tissue indentation or bifurcation and instead, the highest levels of Vangl2 are in cells surrounding the lumen.

These differences in both protein localization and the phenotypes observed following Celsr1 MO knockdown indicate that these proteins have distinct and independent functions in some aspects of lung branching morphogenesis. Although it is possible that these differences may be a consequence of additional roles of these genes outside the PCP pathway, to date, no such additional roles have been attributed to Vangl2 or Celsr1 making this possibility less likely. Using histology, molecular markers and analysis of *Celsr1* and *Vangl2* mouse mutants, we conclude that though both are obligatory for normal lung development, these proteins regulate some distinct steps in airway formation.

Celsr1 is required for bud bifurcation

One mechanism of bud bifurcation previously proposed involves newly synthesized extracellular matrix being deposited transiently and focally in forming cleft regions (59,60). At these points, the extracellular matrix is thought to act as a 'rock in the river' by which the middle of the expanded bud is constrained in position and the bud then bifurcates and flows around this rock to form two new buds. Our data on Celsr1 protein localization show that Celsr1 becomes localized to regions where bud growth is constrained, resembling a 'rope' which tethers the cells at the constriction point or 'rock'. We therefore propose that Celsr1 is required for bud bifurcation; this idea is supported by defects in bifurcation that we observed following morpholino knockdown of Celsr1. Studies of salivary gland branching suggests that laminin may also be a component of the constriction point and its expression shows an intriguing similarity to the Celsr1 'rope' that we observe in the lung endoderm cultures (60). Celsr1 may play an active role in constraining the bifurcation event or may function as a scaffold protein to localize other proteins to sites of constriction during branching. The finding that Celsr1 is expressed in the basal lamina surrounding the lung epithelium is surprising, given that it is known as a transmembrane protein: however, the protein contains a number of laminin G repeats which may enable interaction with the basement membrane. Finally, time-lapse imaging of Celsr1 morpholino treated lung explants reveals reduced branching and, in particular, inhibition of bud bifurcation providing further evidence that Celsr1 is required for bud bifurcation. These new data expand a molecular explanation for the 'rock in the river' model as a mechanism to split the expanded bud into two.

In conclusion, we show for the first time that PCP signalling pathway components are required for normal lung branching morphogenesis *in vivo*. On the basis of our analysis of *Celsr1*^{Crsh} and *Vangl2*^{Lp} mutant mice demonstrating disrupted lung development and cytoskeletal defects, as well as detailed Celsr1 and Vangl2 protein localization data, we propose that the PCP pathway is required for formation of normal epithelial branches in the lung. In addition, our protein localization and

morpholino knockdown data lead us to further propose that Celsr1 is required for bud bifurcation.

We propose that in lung branching morphogenesis, components of the PCP signalling pathway regulate morphogenetic movement of epithelial tissue, at least in part via Rho kinase-mediated regulation of the cytoskeleton. The discovery that *Celsr1* and *Vangl2* are required for lung epithelial tube formation opens up a new avenue of research that will likely increase our understanding of human diseases; particularly those involving defects in lung architecture such as pulmonary fibrosis. To this end, an important part of our future studies will be to determine the roles of Celsr1 and Vangl2 in the postnatal lung using conditional mouse mutants.

MATERIALS AND METHODS

Mouse strains and genotyping

Vangl2^{Lp} mice (Murdoch *et al*., 27) were maintained on C3H/HeH, *Celsr1*^{Crsh} mice (26) were maintained on BALB/C or C3H/HeH. *Vangl2*^{Lp} homozygotes and heterozygotes were identified by craniorachischisis and looped tail phenotypes, respectively, littermates were used as controls. *Crsh* mice and embryos were genotyped for the mutation itself by pyrosequencing, primer sequences available on request. Comparison of limb development in wild-type and homozygous mutant embryos revealed no overall developmental delay.

Antibodies, immunostaining and immunoblotting

Four micrometre paraffin sections or 10 μm cryosections were stained with haematoxylin and eosin or immunostained (61) using antibodies to: Celsr1 1:1000, gift from C. Formstone, manuscript in preparation (caroline.formstone@kcl.ac.uk); Vangl2 1:500, gift from M. Montcouquiol; ZO-2 1:200, PKCζ 1:100, both Santa Cruz; rhodamine phalloidin 1:40 Invitrogen; pan-cytokeratin 1:500; non-muscle myosin IIA 1:1200; β-catenin 1:500; GM-130 1:1500, all Sigma; pro-SP-C 1:1000; Laminin A chain 1:500, both Chemicon; alpha smooth muscle actin 1:1000 Lab Vision; phosphoERK1/2 1:500 Biosource; phospho-histone H3 (pH3) 1:500 Upstate Cell Signaling; p44/42 MAP kinase 1:500, Cell Signaling Technology. Incubations were overnight at 4°C. Pre-incubation for 10 min with −20°C methanol was carried out for phospho-ERK1/2. Antibodies were detected with appropriate Alexa Fluor 488 or 594 secondary antibodies, 1:500 Invitrogen, or with ABC elite staining kit (Vector Labs).

Immunoblotting for ERK proteins was performed using either 18 μg/lane of E12.5 wild-type and *Vangl2*^{Lp} or 7 μg/lane of E13.5 wild-type and *Celsr1*^{Crsh} whole lung protein extract with antibodies to total ERK (1:500), phosphoERK1/2 (1:1000) and β-tubulin (1:5000). For PCP proteins, extract from two morpholino-treated lung explants were loaded/lane immunoblotted for β-actin (1:1000) or Celsr1 (1:3000).

Whole lung immunostaining

E12.5 and E14.5 wild-type and *Celsr1*$^{Crsh/Crsh}$ and *Vangl2*$^{Lp/Lp}$ lungs were fixed in 4% paraformaldehyde (PFA) at 4°C for 1 h. Lungs were washed in PBT and blocked in 5% FCS/PBS/0.1% Triton X-100 and incubated overnight at 4°C with either anti-Celsr1 1:1000 or anti-Vangl2 1:500 and anti-Cytokeratin 1:500, before detection with an appropriate secondary. Lungs were imaged using a Leica TCS SP5 confocal.

Explant cultures

Left lung lobes were isolated from E11.5 mice (wild-type tissue obtained from FVB/N, CD1 or C3H-HeH mice) and cultured for 48 h in defined medium as described (61), or in 1:1 DMEM:F12 (Sigma) containing penicillin-streptomycin (Sigma) and 0.01% bovine serum albumin (BSA, Sigma). In some cases the media was supplemented with FGF10 (400 ng/ml, R&D systems), Rho kinase inhibitor Y27632 (37) (10−30 μM) or Rho kinase activator CNF-1 (20 ng/ml, gift from K. Aktories and G. Schmidt). Following culture, explants were fixed in 4% PFA, and photographed using a Leica digital camera and imaging software. The number of end buds at $t = 48$ varies depending on the precise age of the lung at explant and the strain of mice used. In all experiments control and treated or wild-type and mutant lungs were stage matched at the start of experiments. For explants of lung endoderm, left lung lobes were removed from E11.5 mice and placed in 0.2% trypsin on ice for 45 min. Following removal of the mesenchyme, explants were placed in growth factor reduced matrigel (BD Biosciences) diluted 1:1 in DMEM:F12 containing penicillin-streptomycin and 0.01% BSA and cultured for up to 48 h in the same medium, in some cases, media was supplemented with 400 ng/ml FGF10. Photographs were taken at $t = 0$, 24 and 48 h. At 48 h, explants were fixed with 4% PFA, released from Matrigel and the number of terminal buds counted.

Morpholino knock-down of Celsr1 function

Intact lungs from transgenic mice expressing GFP from the beta-actin promoter (62) were dissected from E11.5 embryos and cultured as described (Dean *et al*., 61). Specific morpholino oligonucleotides (Gene Tools) against Celsr1 (AGCAC AATCCATGCACCCGGCGCAC) or (TCCTGCCCACAGG CCACTCACCTGA) or control (CCTCTTACCTCAGTTAC AATTTATA) were added to the media at final concentration of 15 μM at day zero (Dean *et al*., 61). Lung explants were cultured for 48 h and then images taken every 4 min over a period of 24 h on a Zeiss LSM 510 confocal microscope.

Statistical analysis

All statistics were computed using Excel and Graphpad software. Fluorescent intensity analysis was performed on confocal images using the LSM software. Error bars represent standard error of mean and significance was scored using unpaired two-tailed *t*-tests.

SUPPLEMENTARY MATERIAL

Supplementary Material is available at *HMG* online.

ACKNOWLEDGEMENTS

We thank K. Aktories and G. Schmidt for CNF-1 and M. Montcouquiol for Vangl2 antibody. We also thank histology and imaging at MRC Harwell, particularly Steve Thomas.

Conflict of Interest statement. None declared.

FUNDING

This work was supported by the Medical Research Council, a Sandler Program for Asthma Research (SPAR) award (L.N. and C.D.), NIH R21 HL089431 (L.N.), a fellowship from the British Lung Foundation (C.D.) and a Medical Research Council Career Development Award (J.M.). Funding to pay the Open Access publication charges for this article was provided by the Medical Research Council.

REFERENCES

1. Jancelewicz, T., Nobuhara, K. and Hawgood, S. (2008) Laser microdissection allows detection of abnormal gene expression in cystic adenomatoid malformation of the lung. *J. Pediatr. Surg.*, **43**, 1044–1051.
2. Thebaud, B. and Abman, S.H. (2007) Bronchopulmonary dysplasia: where have all the vessels gone? Roles of angiogenic growth factors in chronic lung disease. *Am. J. Respir. Crit. Care Med.*, **175**, 978–985.
3. Whitsett, J.A., Wert, S.E. and Trapnell, B.C. (2004) Genetic disorders influencing lung formation and function at birth. *Hum. Mol. Genet.*, **13 Spec no. 2**, R207–R215.
4. Chapman, H.A. (2004) Disorders of lung matrix remodeling. *J. Clin. Invest.*, **113**, 148–157.
5. Kimura, J. and Deutsch, G.H. (2007) Key mechanisms of early lung development. *Pediatr. Dev. Pathol.*, **10**, 335–347.
6. Maeda, Y., Dave, V. and Whitsett, J.A. (2007) Transcriptional control of lung morphogenesis. *Physiol. Rev.*, **87**, 219–244.
7. Cardoso, W.V. and Lu, J. (2006) Regulation of early lung morphogenesis: questions, facts and controversies. *Development*, **133**, 1611–1624.
8. Kumar, V.H., Lakshminrusimha, S., El Abiad, M.T., Chess, P.R. and Ryan, R.M. (2005) Growth factors in lung development. *Adv. Clin. Chem.*, **40**, 261–316.
9. Moore, K.A., Huang, S., Kong, Y., Sunday, M.E. and Ingber, D.E. (2002) Control of embryonic lung branching morphogenesis by the Rho activator, cytotoxic necrotizing factor 1. *J. Surg. Res.*, **104**, 95–100.
10. Moore, K.A., Polte, T., Huang, S., Shi, B., Alsberg, E., Sunday, M.E. and Ingber, D.E. (2005) Control of basement membrane remodeling and epithelial branching morphogenesis in embryonic lung by Rho and cytoskeletal tension. *Dev. Dyn.*, **232**, 268–281.
11. Komiya, Y. and Habas, R. (2008) Wnt signal transduction pathways. *Organogenesis*, **4**, 68–75.
12. Marlow, F., Topczewski, J., Sepich, D. and Solnica-Krezel, L. (2002) Zebrafish Rho kinase 2 acts downstream of Wnt11 to mediate cell polarity and effective convergence and extension movements. *Curr. Biol.*, **12**, 876–884.
13. Maddala, R., Reddy, V.N., Epstein, D.L. and Rao, V. (2003) Growth factor induced activation of Rho and Rac GTPases and actin cytoskeletal reorganization in human lens epithelial cells. *Mol. Vis.*, **9**, 329–336.
14. Schlessinger, K., Hall, A. and Tolwinski, N. (2009) Wnt signaling pathways meet Rho GTPases. *Genes. Dev.*, **23**, 265–277.
15. Wojciak-Stothard, B. and Ridley, A.J. (2002) Rho GTPases and the regulation of endothelial permeability. *Vascul. Pharmacol.*, **39**, 187–199.
16. Morrisey, E.E., Hogan and Brigid, L.M. (2010) Preparing for the first breath: genetic and cellular mechanisms in lung development. *Dev. Cell.*, **18**, 8–23.
17. Adler, P.N. (2002) Planar signaling and morphogenesis in *Drosophila*. *Dev. Cell.*, **2**, 525–535.
18. Seifert, J.R. and Mlodzik, M. (2007) Frizzled/PCP signalling: a conserved mechanism regulating cell polarity and directed motility. *Nat. Rev. Genet.*, **8**, 126–138.
19. Barrow, J.R. (2006) Wnt/PCP signaling: a veritable polar star in establishing patterns of polarity in embryonic tissues. *Semin. Cell Dev. Biol.*, **17**, 185–193.
20. Jenny, A. and Mlodzik, M. (2006) Planar cell polarity signaling: a common mechanism for cellular polarization. *Mt. Sinai. J. Med.*, **73**, 738–750.
21. Karner, C., Wharton, K.A. Jr and Carroll, T.J. (2006) Planar cell polarity and vertebrate organogenesis. *Semin. Cell. Dev. Biol.*, **17**, 194–203.
22. Vandenberg, A.L. and Sassoon, D.A. (2009) Non-canonical Wnt signaling regulates cell polarity in female reproductive tract development via van gogh-like 2. *Development*, **136**, 1559–1570.
23. Bastock, R. and Strutt, D. (2007) The planar polarity pathway promotes coordinated cell migration during *Drosophila* oogenesis. *Development*, **134**, 3055–3064.
24. Karner, C.M., Chirumamilla, R., Aoki, S., Igarashi, P., Wallingford, J.B. and Carroll, T.J. (2009) Wnt9b signaling regulates planar cell polarity and kidney tubule morphogenesis. *Nat. Genet.*, **41**, 793–799.
25. Copp, A.J., Greene, N.D. and Murdoch, J.N. (2003) Dishevelled: linking convergent extension with neural tube closure. *Trends Neurosci.*, **26**, 453–455.
26. Curtin, J.A., Quint, E., Tsipouri, V., Arkell, R.M., Cattanach, B., Copp, A.J., Henderson, D.J., Spurr, N., Stanier, P., Fisher, E.M. *et al.* (2003) Mutation of Celsr1 disrupts planar polarity of inner ear hair cells and causes severe neural tube defects in the mouse. *Curr. Biol.*, **13**, 1129–1133.
27. Murdoch, J.N., Doudney, K., Paternotte, C., Copp, A.J. and Stanier, P. (2001) Severe neural tube defects in the loop-tail mouse result from mutation of Lpp1, a novel gene involved in floor plate specification. *Hum. Mol. Genet.*, **10**, 2593–2601.
28. Murdoch, J.N., Henderson, D.J., Doudney, K., Gaston-Massuet, C., Phillips, H.M., Paternotte, C., Arkell, R., Stanier, P. and Copp, A.J. (2003) Disruption of scribble (Scrb1) causes severe neural tube defects in the circletail mouse. *Hum. Mol. Genet.*, **12**, 87–98.
29. Torban, E., Kor, C. and Gros, P. (2004) Van Gogh-like2 (Strabismus) and its role in planar cell polarity and convergent extension in vertebrates. *Trends. Genet.*, **20**, 570–577.
30. Kibar, Z., Vogan, K.J., Groulx, N., Justice, M.J., Underhill, D.A. and Gros, P. (2001) Ltap, a mammalian homolog of *Drosophila* Strabismus/Van Gogh, is altered in the mouse neural tube mutant Loop-tail. *Nat. Genet.*, **28**, 251–255.
31. Wang, J., Hamblet, N.S., Mark, S., Dickinson, M.E., Brinkman, B.C., Segil, N., Fraser, S.E., Chen, P., Wallingford, J.B. and Wynshaw-Boris, A. (2006) Dishevelled genes mediate a conserved mammalian PCP pathway to regulate convergent extension during neurulation. *Development*, **133**, 1767–1778.
32. Ybot-Gonzalez, P., Savery, D., Gerrelli, D., Signore, M., Mitchell, C.E., Faux, C.H., Greene, N.D. and Copp, A.J. (2007) Convergent extension, planar-cell-polarity signalling and initiation of mouse neural tube closure. *Development*, **134**, 789–799.
33. Laudy, J.A. and Wladimiroff, J.W. (2000) The fetal lung. 1: developmental aspects. *Ultrasound Obstet. Gynecol.*, **16**, 284–290.
34. Metzger, R.J., Klein, O.D., Martin, G.R. and Krasnow, M.A. (2008) The branching programme of mouse lung development. *Nature*, **453**, 745–750.
35. Wei, L., Roberts, W., Wang, L., Yamada, M., Zhang, S., Zhao, Z., Rivkees, S.A., Schwartz, R.J. and Imanaka-Yoshida, K. (2001) Rho kinases play an obligatory role in vertebrate embryonic organogenesis. *Development*, **128**, 2953–2962.
36. Fanto, M., Weber, U., Strutt, D.I. and Mlodzik, M. (2000) Nuclear signaling by Rac and Rho GTPases is required in the establishment of epithelial planar polarity in the *Drosophila* eye. *Curr. Biol.*, **10**, 979–988.
37. Uehata, M., Ishizaki, T., Satoh, H., Ono, T., Kawahara, T., Morishita, T., Tamakawa, H., Yamagami, K., Inui, J., Maekawa, M. *et al.* (1997) Calcium sensitization of smooth muscle mediated by a Rho-associated protein kinase in hypertension. *Nature*, **389**, 990–994.
38. Lerm, M., Schmidt, G., Goehring, U.M., Schirmer, J. and Aktories, K. (1999) Identification of the region of rho involved in substrate recognition by Escherichia coli cytotoxic necrotizing factor 1 (CNF1). *J. Biol. Chem.*, **274**, 28999–29004.

39. Amano, M., Ito, M., Kimura, K., Fukata, Y., Chihara, K., Nakano, T., Matsuura, Y. and Kaibuchi, K. (1996) Phosphorylation and activation of myosin by Rho-associated kinase (Rho-kinase). *J. Biol. Chem.*, **271**, 20246–20249.
40. Liu, Y., Stein, E., Oliver, T., Li, Y., Brunken, W.J., Koch, M., Tessier-Lavigne, M. and Hogan, B.L. (2004) Novel role for Netrins in regulating epithelial behavior during lung branching morphogenesis. *Curr. Biol.*, **14**, 897–905.
41. Devenport, D. and Fuchs, E. (2008) Planar polarization in embryonic epidermis orchestrates global asymmetric morphogenesis of hair follicles. *Nat. Cell Biol.*, **10**, 1257–1268.
42. Mollard, R. and Dziadek, M. (1998) A correlation between epithelial proliferation rates, basement membrane component localization patterns, and morphogenetic potential in the embryonic mouse lung. *Am. J. Respir. Cell Mol. Biol.*, **19**, 71–82.
43. Torban, E., Wang, H.J., Patenaude, A.M., Riccomagno, M., Daniels, E., Epstein, D. and Gros, P. (2007) Tissue, cellular and sub-cellular localization of the Vangl2 protein during embryonic development: effect of the Lp mutation. *Gene Expr. Patterns*, **7**, 346–354.
44. Habas, R., Kato, Y. and He, X. (2001) Wnt/Frizzled activation of Rho regulates vertebrate gastrulation and requires a novel Formin homology protein Daam1. *Cell*, **107**, 843–854.
45. Strutt, D.I., Weber, U. and Mlodzik, M. (1997) The role of RhoA in tissue polarity and Frizzled signalling. *Nature*, **387**, 292–295.
46. Quaggin, S.E., Schwartz, L., Cui, S., Igarashi, P., Deimling, J., Post, M. and Rossant, J. (1999) The basic-helix-loop-helix protein pod1 is critically important for kidney and lung organogenesis. *Development*, **126**, 5771–5783.
47. Kaartinen, V., Voncken, J.W., Shuler, C., Warburton, D., Bu, D., Heisterkamp, N. and Groffen, J. (1995) Abnormal lung development and cleft palate in mice lacking TGF-beta 3 indicates defects of epithelial-mesenchymal interaction. *Nat. Genet.*, **11**, 415–421.
48. Gontan, C., de Munck, A., Vermeij, M., Grosveld, F., Tibboel, D. and Rottier, R. (2008) Sox2 is important for two crucial processes in lung development: branching morphogenesis and epithelial cell differentiation. *Dev. Biol.*, **317**, 296–309.
49. De Langhe, S.P., Sala, F.G., Del Moral, P.M., Fairbanks, T.J., Yamada, K.M., Warburton, D., Burns, R.C. and Bellusci, S. (2005) Dickkopf-1 (DKK1) reveals that fibronectin is a major target of Wnt signaling in branching morphogenesis of the mouse embryonic lung. *Dev. Biol.*, **277**, 316–331.
50. Miettinen, P.J., Warburton, D., Bu, D., Zhao, J.S., Berger, J.E., Minoo, P., Koivisto, T., Allen, L., Dobbs, L., Werb, Z. *et al.* (1997) Impaired lung branching morphogenesis in the absence of functional EGF receptor. *Dev. Biol.*, **186**, 224–236.
51. Fischer, E., Legue, E., Doyen, A., Nato, F., Nicolas, J.F., Torres, V., Yaniv, M. and Pontoglio, M. (2006) Defective planar cell polarity in polycystic kidney disease. *Nat. Genet.*, **38**, 21–23.
52. Ross, A.J., May-Simera, H., Eichers, E.R., Kai, M., Hill, J., Jagger, D.J., Leitch, C.C., Chapple, J.P., Munro, P.M., Fisher, S. *et al.* (2005) Disruption of Bardet-Biedl syndrome ciliary proteins perturbs planar cell polarity in vertebrates. *Nat. Genet.*, **37**, 1135–1140.
53. Simons, M., Gloy, J., Ganner, A., Bullerkotte, A., Bashkurov, M., Kronig, C., Schermer, B., Benzing, T., Cabello, O.A., Jenny, A. *et al.* (2005) Inversin, the gene product mutated in nephronophthisis type II, functions as a molecular switch between Wnt signaling pathways. *Nat. Genet.*, **37**, 537–543.
54. Henderson, D.J., Phillips, H.M. and Chaudhry, B. (2006) Vang-like 2 and noncanonical Wnt signaling in outflow tract development. *Trends Cardiovasc. Med.*, **16**, 38–45.
55. Phillips, H.M., Rhee, H.J., Murdoch, J.N., Hildreth, V., Peat, J.D., Anderson, R.H., Copp, A.J., Chaudhry, B. and Henderson, D.J. (2007) Disruption of Planar cell polarity signaling results in congenital heart defects and cardiomyopathy attributable to early cardiomyocyte disorganization. *Circ. Res.*, **101**, 137–145.
56. Dow, L.E., Kauffman, J.S., Caddy, J., Zarbalis, K., Peterson, A.S., Jane, S.M., Russell, S.M. and Humbert, P.O. (2007) The tumour-suppressor Scribble dictates cell polarity during directed epithelial migration: regulation of Rho GTPase recruitment to the leading edge. *Oncogene*, **26**, 2272–2282.
57. Zhou, W., Lin, L., Majumdar, A., Li, X., Zhang, X., Liu, W., Etheridge, L., Shi, Y., Martin, J., Van de Ven, W. *et al.* (2007) Modulation of morphogenesis by noncanonical Wnt signaling requires ATF/CREB family-mediated transcriptional activation of TGFbeta2. *Nat. Genet.*, **39**, 1225–1234.
58. Kalabis, J., Rosenberg, I. and Podolsky, D.K. (2006) Vangl1 protein acts as a downstream effector of intestinal trefoil factor (ITF)/TFF3 signaling and regulates wound healing of intestinal epithelium. *J. Biol. Chem.*, **281**, 6434–6441.
59. Sakai, T., Larsen, M. and Yamada, K.M. (2003) Fibronectin requirement in branching morphogenesis. *Nature*, **423**, 876–881.
60. Rebustini, I.T., Patel, V.N., Stewart, J.S., Layvey, A., Georges-Labouesse, E., Miner, J.H. and Hoffman, M.P. (2007) Laminin alpha5 is necessary for submandibular gland epithelial morphogenesis and influences FGFR expression through beta1 integrin signaling. *Dev. Biol.*, **308**, 15–29.
61. Dean, C.H., Miller, L.A., Smith, A.N., Dufort, D., Lang, R.A. and Niswander, L.A. (2005) Canonical Wnt signaling negatively regulates branching morphogenesis of the lung and lacrimal gland. *Dev. Biol.*, **286**, 270–286.
62. Hadjantonakis, A.K., Gertsenstein, M., Ikawa, M., Okabe, M. and Nagy, A. (1998) Non-invasive sexing of preimplantation stage mammalian embryos. *Nat. Genet.*, **19**, 220–222.